A NEW, SIMPLE AND EXACT RESULT FOR CALCULATING THE PROBABILITY OF ERROR FOR TWO-DIMENSIONAL SIGNAL CONSTELLATIONS

John W. Craig
Interstate Electronics Corporation
1001 East Ball Road
P. O. Box 3117
Anaheim, CA 92803
Phone: (714) 758-0500

Abstract

In most signaling schemes in digital communication, the boundaries of the decision regions are straight lines. For some of these schemes such as quadrature amplitude modulation and its special cases where the boundaries meet at right angles, simple and exact expressions are known for the probability of error on an AWGN channel. In other cases where the boundaries do not meet at right angles, the exact expressions contain integrals of special functions which are often difficult to evaluate. Examples of these are M-ary phase shift keying (MPSK) and the wide variety of QAM and AMPM constellations of signal points, among many others. Here by expressing the double integral for the probability of error (PE) in a different way than has been done before, we show that the PE can be expressed as the sum of a small number of simple, single integrals, all with the same integrand containing only elementary functions and all having a finite range. Applied to MPSK, this approach gives just one simple, finite integral for PE, and the values of PE so obtained are in excellent agreement with those tabulated by Lindsey and Simon in their book *Telecommunication Systems Engineering*. Numerical results for these and other signal constellations of interest will be presented in the paper. This approach is applicable to any set of signal points having polygonal decision regions. An interesting related result is that this approach gives a new and simple integral expression for the Gaussian tail probability function Q(x), and by the same token, a similar result for the complementary error function erfc(x).

I. Introduction

Union bounds are widely used to calculate probability of error for a large variety of signal constellations, and the results are perfectly satisfactory for the very low error rates at high signal-to-noise ratio (SNR). At low and moderate SNRs there appears to be no general method for the exact calculation of probability of error for an arbitrary array of signal points. However, for the special case of quadrature amplitude modulation with a square constellation of signal points, a simple and exact expression is known. Also, for MPSK two exact expressions are known, but both require high accuracy in the numerical evaluation of integrals involving the error function. Here we present a new approach that gives simple expressions for the exact probability of symbol error for any array of signal points, and apply it to MPSK and several 16-point signal constellations of general interest. The integrals required in these expressions are all of the same form, involve only elementary functions, and have a finite range.

In section II the approach is introduced by applying it to MPSK. The special case of M = 2 gives new and possibly useful expressions for calculating the Gaussian tail probability function Q(x) and the related complementary error function erfc(x). Section III outlines the approach for polygonal decision regions, and section IV illustrates the approach and gives results for the 16-point signal constellations. Section V presents a way of obtaining, not exact, but even simpler and highly accurate expressions for symbol error probability when the latter is less than a few hundredths. Section VI has a concise summary.

II. Probability of Error for MPSK - A New Look

In this section a new and simple expression is presented for the exact probability of error of M-ary PSK. The expression is an integral over a finite range of an integrand containing only elementary functions. It is also shown that the widely used approximate expression for the probability of error is very accurate indeed, even at probabilities as high as 10^{-3} to 10^{-2}.

Figure 1 shows one signal point, S_n, and its decision region for MPSK. An error is made if noise causes the matched filter detector output to be outside the wedge-shaped decision region bounded by the semi-infinite lines OA and OC, as for example the point Z. The probability of a symbol error, P_M, is twice the probability that Z lies above the boundary AOD.

So

$$P_M = 2 \int_0^{\pi-\Psi} d\theta \int_R^{\infty} p(r,\theta)\, dr \qquad (1)$$

where R is the distance from the signal point to the boundary point E, and $p(r,\theta)$ is the bivariate Gaussian density function expressed in polar coordinates. For the assumed additive, narrow band, white Gaussian noise having independent in-phase and quadrature components, $p(r,\theta)$ is

$$p(r,\theta) = \frac{r}{2\pi\sigma^2} \exp\left(-\frac{r^2}{2\sigma^2}\right). \qquad (2)$$

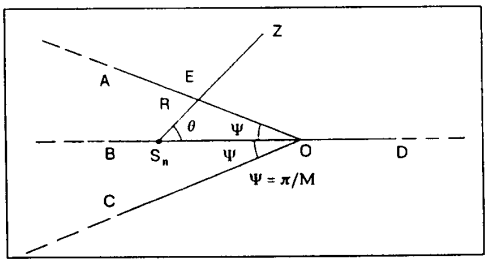

Figure 1. The decision region for one signal point S_n in MPSK is the wedge AOC. The point Z is at a distance r from S_n.

CH2981-9/91/0000-0571 $1.00 © 1991 IEEE

Substituting (2) into (1) and carrying out the integration on r gives

$$P_M = \frac{1}{\pi} \int_0^{\pi-\Psi} \exp\left[-\frac{X_0^2 \sin^2(\Psi)}{2\sigma^2 \sin^2(\theta + \Psi)}\right] d\theta \qquad (3)$$

where, the law of sines

$$R = \frac{X_0 \sin(\Psi)}{\sin(\theta + \Psi)} \qquad (4)$$

has been used. For the matched filter detector, it is easy to show that $X_0^2/2\sigma^2$ is just the symbol energy E_s divided by the noise density No, which will be called γ_s. After the change of variable $\phi = \pi - (\theta + \Psi)$, the final form of P_M is obtained:

$$P_M = \frac{1}{\pi} \int_0^{\pi-\Psi} \exp\left[-\frac{\gamma_s \sin^2(\Psi)}{\sin^2(\Phi)}\right] d\Phi. \qquad (5)$$

The simplicity of this result is to be compared with the more complex forms given in the books by Lindsey and Simon[1] and by Proakis[2]. There are two advantages of this new result over the previous expressions. First, the integrand in (5) contains only elementary functions whereas those in the cited expressions contain the error function so the former is easier to evaluate. Also, (5) gives the probability of error directly while the other expressions require the value of a more complicated integral to be subtracted from a constant near unity, so for the same resultant accuracy, fewer significant figures are required in the numerical evaluation of (5) than for the more complex integrals. For small probability of error, the difference is quite significant.

As a proof of the validity of this new expression for P_M, the integral in (5) was evaluated using a Gauss-Legendre quadrature formula[3] for many values of γ_s and for M = 2 through 64, and the results were compared with the table of values for P_M in Lindsey and Simon[1], pp. 232-3. All pairs of values agreed to at least five significant figures (except for a few of the lowest PM in the table) so the validity of (5) is established. This also shows the care that was used by Lindsey and Simon in calculating the table.

An Approximate Expression for P_M

An accurate and widely used approximate expression for P_M is given by Proakis[2], p. 169, which is

$$P_M \approx \text{erfc}\left(\sqrt{\gamma_s}\sin(\pi/M)\right) = 2Q\left(\sqrt{2\gamma_s}\sin(\pi/M)\right) \qquad (6)$$

where

$$\gamma_s = \gamma_b \log_2(M). \qquad (7)$$

This result is valid for $M = 2^k$ with k an integer greater than or equal to two. For M = 2 the geometry of the decision regions degenerates to cause (6) to be too large by a factor of two. For M = 2, the exact result is

$$P_2 = Q\left(\sqrt{2\gamma_b}\right) = \frac{1}{2}\text{erfc}\left(\sqrt{\gamma_b}\right). \qquad (8)$$

By equating this result to expression (5) for M = 2 ($\Psi = \pi/2$) new expressions for Q(x) and erfc(x) are obtained which are:

$$Q(X) = \frac{1}{\pi} \int_0^{\pi/2} \exp\left(-\frac{X^2}{2\sin^2(\Phi)}\right) d\Phi. \qquad (9)$$

and

$$\text{erfc}(X) = \frac{2}{\pi} \int_0^{\pi/2} \exp\left(-\frac{X^2}{\sin^2(\Phi)}\right) d\Phi. \qquad (10)$$

These expressions are valid for nonnegative values of x, but sometimes Q(x) and erfc(x) are needed for negative x. In the latter case, the following expressions can be used in conjunction with (9) and (10):

$$Q(-x) = 1 - Q(x) \qquad (11)$$

and

$$\text{erfc}(-x) = 2 - \text{erfc}(x) \qquad (12)$$

which are valid for nonnegative x.

Equations (9) and (10) are of interest in and of themselves as new ways of expressing these functions and have the advantage that the range of integration is finite. In a practical sense, they can be used to compute values of these functions even on hand calculators such as the Hewlett-Packard models 15C and 42S that have built-in numerical integration programs. In fact, (9) was verified using a model 15C.

III. Exact Probability of Error for Arbitrary Signal-Point Geometry

For any arbitrary arrangement of signal points and additive Gaussian noise, the boundaries of the decision regions are polygons. Figure 2 shows a typical signal point, S_n, and its four-sided decision region ABCDA. If S_n is transmitted, an error in reception occurs if noise causes the detector to produce a point outside the boundary in regions 1, 2, 3, or 4 which are disjoint. The probability that the detected point lies in region 1 is like the right side of (3) with x_o replaced by x_1, Ψ replaced by Ψ_1, and the upper limit on the integral replaced by Ψ_1. The probability that the detected point lies in any of the other three regions is given by a similar expression. Since the four regions are disjoint and comprise the complete error space, the probability of a symbol error P_{sn} when S_n is transmitted is the sum of the above expressions for the four regions. Thus, P_{sn} is

$$P_{sn} = \frac{1}{\pi} \sum_{k=1}^{4} \int_0^{\theta_k} \left[-\frac{X_k^2 \sin^2(\Psi_k)}{2\sigma^2 \sin^2(\theta + \Psi_k)}\right] d\theta. \qquad (13)$$

The probability of error when another signal point in the constellation is transmitted is like (13) except that the sum might have a different number of terms. For any signal point, the number of terms in the sum for P_{sn} will be equal to the number of sides on its decision region. So now if $P(S_n)$ is the a priori probability that the signal point S_n is transmitted, the probability of a symbol error P_s for a set of N signal points is

$$P_s = \sum_{n=1}^{N} P_{sn}\, P(S_n). \qquad (14)$$

It remains to relate the ratios x_k^2/σ^2 in (13) to the energy per bit to noise density ratio. In general, σ^2 equals $N_o T_{sn}$ where N_o is the one-sided noise density and T_s is the symbol duration. Also, x_k is the distance from one of the signal points to the k^{th} corner of its decision region. Such distances can be related to the location of the signal points and their probabilities of transmission, but such descriptions are beyond the scope of this paper. Therefore, it will be left to specific cases to relate the x_k to a signal parameter of interest, often the average carrier power. It is sufficient here to say that for any set of signal points, the ratio x_k^2/σ^2 can be related to E_b/N_o. Several examples are discussed in the next section. Also, equiprobable signal points are assumed.

IV. Some Signal Point Constellations to Illustrate the Exact Calculation of Probability of Symbol Error

In this section the use of equations (13) and (14) to calculate the probability of symbol error for three 16-point signal constellations is illustrated. These are the 8-pointed star array (also called the (8,8) array), the (4,12) array and the CCITT V.29 array; and they are shown with the decision boundaries for equiprobable signals in figures 3 to 5, respectively. The first two are of interest in communication systems having a nonlinear power amplifier, such as satellite communications. Although they do not have the constant amplitude of unfiltered MPSK (which has amplitude fluctuations after required filtering anyway), they are an attempt to improve performance over MPSK for a fixed-peak signal power by moving the signal points further apart while introducing not too much envelope variation. The earliest reference found to the arrays is Thomas, et al[3]. The third array has been selected by the CCITT as the standard for 9600 bits/sec transmission on telephone lines[4]. Only the (8,8) array is treated in any detail here, but performance curves of symbol error probability versus peak Eb/No for all three are given. In addition, simple but very accurate expressions for P_s are developed. They are based on union bounds and so are an upper limit, but they turn out to be very accurate even at probabilities as high as 10^{-2}. In each case, the a priori probabilities of signals are all equal.

As figure 3 shows, the inner signal points have identical decision regions, as do the outer points, and both have symmetries that can be exploited to simplify the calculation of P_s. The geometry of the regular 8-pointed star is as follows. The eight inner points constitute those of an 8 PSK signal on a circle of radius R_1 with adjacent pairs being a distance $2d_1$ apart. The signals at the points of the star are also placed at a distance $2d_1$ from their nearest neighbors, and they are on a circle of radius R_2 where $R_2 = d_1(1+\sqrt{2}+\sqrt{3})$. In figure 3 the decision region for a signal point is symmetric about a radial line through that point. Thus, the PE can be found from the bisected regions shown in figure 6a for an inner signal point and in figure 6b for an outer signal point. The probability of a symbol error, given that an inner signal point is sent, is twice the probability that noise causes the detector output to be in region 1 or 2 of figure 6a. Similarly, if an outer signal point is sent, the probability of an error is twice the probability that noise causes the detector output to be in region 3 or 4 of figure 6b. Since the probability of transmitting an inner point is one-half, as is that of an outer point, the total probability of a symbol error is the probability that the detector output is in one of the four regions above. These regions being disjoint, the probability of symbol error is the sum of the probabilities for the four regions. For regions 1-3, the total probability is expressed by equation (13) with three terms in the sum. The parameters for each term are identified in figure 6, and their values are given in table I. For the fourth region, the required probability is given by equation (5) with Ψ equal to Ψ_4 and γ_s replaced by $x_4^2/2\sigma^2$ using the values in table I. Note that the parameters for regions 1 and 3 are the same. This is not an accident but is the result of the geometry. Pairs of this sort can always be found for signal points having abutting decision regions, and using them keeps the number of different integrals to a minimum.

Now it is easy to relate the ratio $(x_k/\sigma)^2$ in equation (13) to $\gamma_{b\,max}$, the maximum E_b/N_o, since $\gamma_{b\,max} = R_2^2/8\sigma^2$. Thus, for any values of $\gamma_{b\,max}$ the exact probability of symbol error can be determined by numerically evaluating a few simple

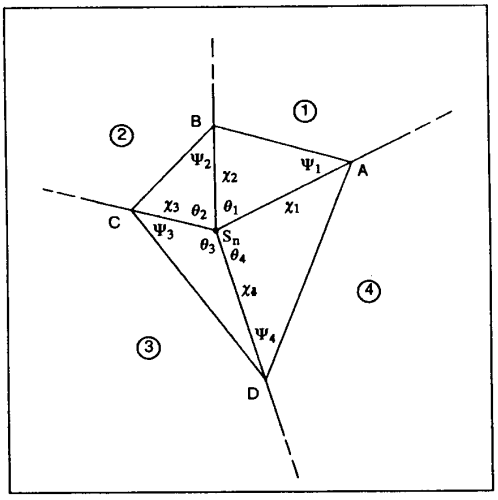

Figure 2. A typical signal point and its decision boundary, assumed four-sided for illustration.

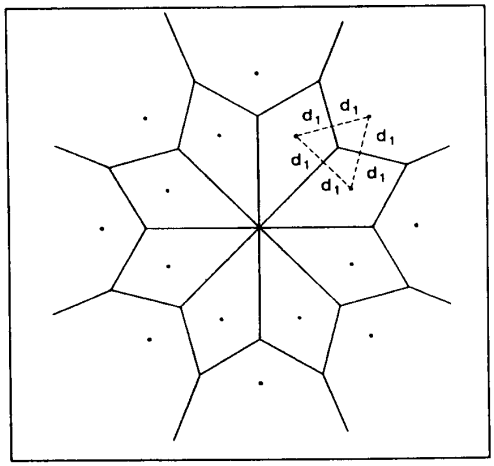

Figure 3. The 8-pointed star or (8,8) array and its decision boundaries.

TABLE I. PARAMETER VALUES FOR THE INTEGRALS IN REGIONS 1-4 IN FIGURE 6

k	x_k	θ_k	ψ_k
1	$0.3962\ R_2$	82.5°	37.5°
2	$0.2785\ R_2$	97.5°	60.0°
3	$0.3962\ R_2$	82.5°	37.5°
4	$0.3962\ R_2$		105.0°

integrals that are determined as in this example. The results of doing so for the four 16-point arrays mentioned above and for 16 QAM are plotted in figure 7, which shows symbol error probability versus maximum E_b/N_o. These show the penalty incurred by 16PSK because of its closely spaced signals, and why it is believed that a (4,12) or (8,8) array might be advantageous on a nonlinear channel.

V. Union Bounds and Their Accuracy

Now that a simple way has been shown to calculate the probability of error exactly, it is useful to determine the accuracy of some union bounds that are widely used. Since these bounds are tight at high SNR, particular attention will be paid to the low SNR range. It is found for the variety of constellations considered here that even at a probability of error as high as 0.01 the bounds give an error in E_b/N_o of less than 0.1 dB.

Union bounds are based on the distances from the various signal points to the sides of their decision boundaries. In a particular constallation, there are a few of these distances (often only one or two) that are significantly smaller than the others. So, rather than using all the distances to form a bound, use only this group of the smallest distances. For a minimum distance dj from a signal point to a side of its decision boundary, the probability of error for this point and side is upper bounded by $Q(d_j/\sigma)$. A bound on the total probability of error is obtained by weighting each $Q(d_j/\sigma)$ by its probability of occurrence and summing over the distances in the smallest distance set. As an example of this, again take the 8-pointed star array. The smallest distance from any signal point to its decision boundary is d_1, and it occurs four times for each inner signal point and twice for each outer one. The next larger such distance is half the distance between adjacent outer signal points which is $R_2 \sin(\pi/8) = 1.587\ d_1$, and this is large enough compared to d_1 to give a negligible contribution. Thus, the proposed bound is based on d_1 only. Taking the probabilities of occurrence into account, the bound on the symbol error rate is

$$P_s \approx 3Q\ (d_1/\sigma) = 3Q\ \left(0.682\sqrt{\gamma_{bmax}}\right). \qquad (15)$$

A comparison between this and the exact result shows equation (15) to be an upper bound, being very tight for $P_s \leq 10^{-3}$ and less than 0.1 dB in error at $P_s = 0.01$.

As a second example, take the (4,12) array in which the twelve outer points are uniformly spaced a distance $2d_o$ apart around a circle of radius R_2, and the four inner points are each at a distance $2d_o$ from two of the outer points as shown in figure 4.

The shortest distance from a signal point to a decision boundary is d_o, and it occurs twice for each inner point, twice for four of the outer points, and three times for eight of the outer points. The next larger distance is $\sqrt{2}\,d_o$ which is large enough to give a negligible contribution to P_s. So an approximation to the symbol error probability for the (4,12) array is

$$P_s \approx 2.5Q(d_o/\sigma) = 2.5Q\ \left(0.732\sqrt{\gamma_{bmax}}\right). \qquad (16)$$

As in the previous example, this result turns out to be an upper bound which is very tight at high SNR and gives less than 0.1 dB error at $P_s = 0.01$.

As the last example of this approximation technique, take the CCITT V.29 array, for which the decision regions in figure 5 have four different shapes. The shortest distance from a signal point to a decision boundary is d_o, and it occurs twice for each of

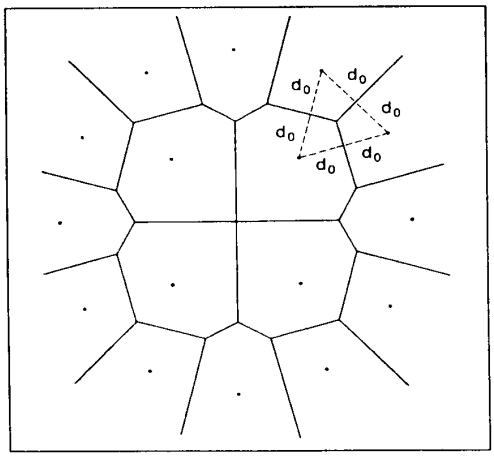

Figure 4. The (4,12) array and its decision boundaries.

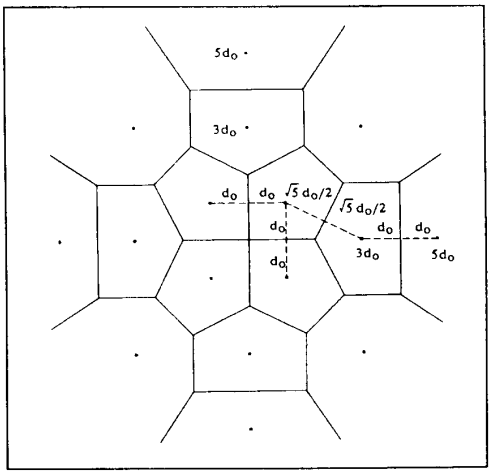

Figure 5. The CCITT V.29 array and its decision boundaries.

the four innermost signal points, once for each of the four points at a distance of $3d_o$ from the center, and also once for each of the four points at a distance of $5d_o$ from the center. The next larger distance is $\sqrt{5}\,d_0/2$ and it is small enough to make an important contribution to the error probability. This distance occurs twice for each of the four innermost points and also twice for each of the four points at a distance $3d_o$ from the center. The next larger distances are $\sqrt{2}\,d_0$ and 1.5 d_o, which are large enough to give insignificant contributions to P_s, so the resulting approximation to the symbol error probability for the CCITT V.29 array is

$$P_s \approx Q\left(\frac{d_o}{\sigma}\right) + Q\left(\frac{\sqrt{5}\,d_o}{2\sigma}\right) = Q\left(\sqrt{0.32\gamma_{bmax}}\right) + Q\left(\sqrt{0.4\gamma_{bmax}}\right). \quad (17)$$

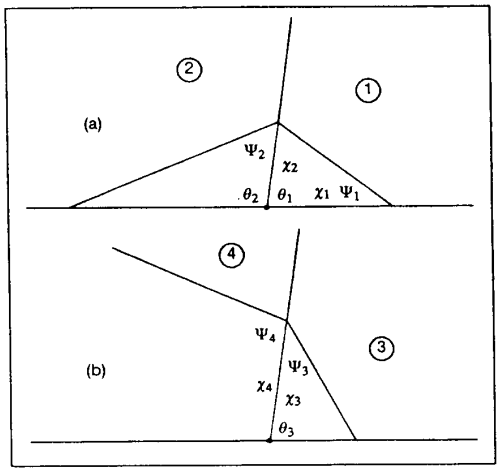

Figure 6. The bisected decision regions of the 8-pointed star array.

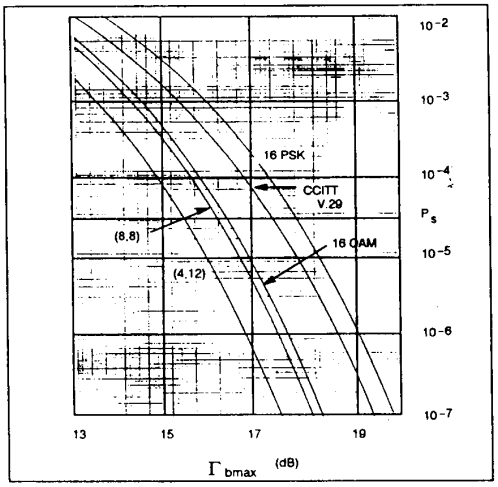

Figure 7. Symbol error probability versus maximum E_b / N_o in dB for several 16-point signal constellations.

Comparison of results from this approximate expression to the exact values shows that equation (17) is an upper bound for P_s less than 0.022, and that it is accurate to less than 0.1 dB for P_s less than 0.07. As with the previous approximations, (15 and (16), equation (17) is very tight at high SNR.

These results suggest the conjecture that similar, simple but very accurate approximate expressions for the probability of symbol error can be found for any array of signal points, and furthermore that the range of P_s for this accuracy is $P_s < 0.01$, which is the range of most practical interest.

VI. Conclusions

In this paper we have presented a simple integral expression for calculating the exact probability of a symbol error for an arbitrary array of signal points. The integrand contains only elementary functions and the range of integration is finite, so even a hand-held calculator can perform the numerical integration with a minimum of effort. Applied to MPSK, this approach gives a new and much simpler expression for the exact probability of symbol error. Three arrays of sixteen signal points were chosen to illustrate the use of this new expression, and these exact results were used to prove the high accuracy (for $P_s < 0.01$) of simple expressions obtained from modified union bounds. As a collateral result, new expressions were presented for the Guassian tail probability function Q(x) and the closely related complementary error function erfc(x).

References

1. Lindsey, W.C. and Simon, M.K., *Telecommunication Systems Engineering*, Prentice-Hall, Englewood Cliffs, N.J., 1973, p. 231.

2. Proakis, J.G., *Digital Communications*, McGraw-Hill, New York, N.Y., 1983, pp. 167-8.

3. Ralston, A., and Rabinowitz, P., *A First Course in Numerical Analysis*, 2nd ed., McGraw-Hill, New York, N.Y., 1978, p. 116.

4. Thomas, C.M., Weidner, M.Y. and Durrani, S.H., "Digital Amplitude - Phase Keying with M-ary Alphabets," *IEEE Trans. Commun.*, vol. COM-22, pp. 168-179, Feb. 1974.

5. Lee, E.A. and Messerschmitt, D.G., *Digital Communication*, Kluwer, Boston, 1988, p. 243.